PINSA, **67, A,** Nos. 4 & 5, July & September 2001, pp. 461-478.
© Printed in India

VIBRATION DAMPING

B C NAKRA

Mechanical Engineering Department, Indian Institute of Technology, Hauz Khas, New Delhi- 110016 (India)

(Received 28 January 2000; After Revision 28 April 2000; Accepted 25 August 2000)

The damping mechanisms in materials and their characterisation are reviewed for viscous, hysteretic, coulomb and viscoelastic types of damping. The techniques for determination of damping characteristics and the influence of parameters like frequency, temperature and strain are outlined. Analysis and characteristics of various additive damping methods like surface damping techniques including constrained and unconstrained layer damping methods and concentrated damping methods are discussed. The influence of damping on the dynamic behaviour of machines and structures is highlighted. The use of damping technology for vibration control over a wide frequency range for applications in machines and structures, is brought out. Current work on dynamic design involving multi-parameter optimisation, structural dynamic modification and active damping are reported and emerging trends are discussed.

Key Words: Vibrations; Damping; Viscoelastic Damping Technology; Unconstrained and Constrained Treatment; Dynamic Design; Active Control

1 Introduction

The subject of vibration damping has acquired importance from point of view of vibrations and noise control in structures and machines and has received considerable attention over the past several decades. Vibration control has been carried out by several means including reduction of excitations, avoiding of resonance by proper choice of stiffness and mass parameters, use of vibration absorbers and dampers. The dampers are of viscous damping type, coulomb damping, material or hysteretic damping types using conventional materials. For vibration control over a wide frequency range as in aero-space, automotive and other applications, the above methods have limitations and the use of viscoelastic damping involving use of polymeric or elastomeric materials is finding considerable importance. Efforts to develop metallic alloys with high damping do not appear to have yielded encouraging results. The use of active damping is also being investigated for applications in such situations.

Internal or hysteretic damping is due to internal friction in materials caused by a number of combination of physical mechanisms[1,2]. In metals, it may be due to thermoelasticity, grain boundary viscosity, point defect relaxation, eddy current effects, stress induced ordering, electronic effects etc. In case of polymeric or long order molecules, rheological behaviour results in damping while in case of composite materials, the mechanism of damping is due to microplastic or viscoelastic phenomena associated with the matrix and reinforcement. Due to internal damping in the various materials, the hysteresis loops between stress and strain are obtained as in Fig. 1, with the area giving the energy dissipated per cycle in the material.

Coulomb, as early as 1784 felt that the damping is due to internal losses in materials and the damping mechanism at low stresses may be different from that at high stresses. According to Lazan[1], in this area, there were only 70 papers in this subject till 1920. The total number of papers was only about 500 till 1945 and 2000 till 1960. Since then, the number has been doubling every 9 years[1]. Much of the later work concerns characterisation of damping in viscoelastic materials and arrangements involving suitable combinations of elastic and viscoelastic materials. It may be seen that material damping is

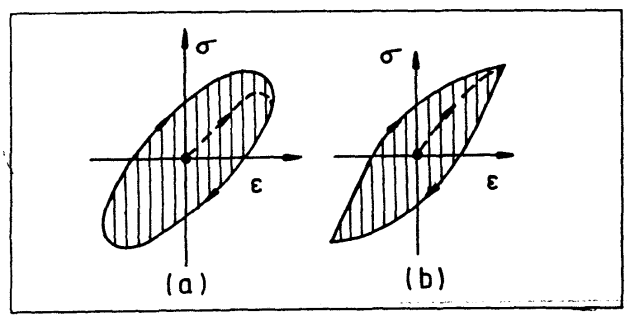

Fig. 1 Hysteresis loops a) Linear materials b) Non-linear materials – metals at high stress

significant not only from vibration and noise control point of view but also from point of view of stability of rotating systems and flutter of aero-space structures.

In the present paper, methods for characterisation and determination of the damping properties of materials, analysis and use of viscoelastic damping technology and current trends in the use of active and hybrid vibration damping methods are outlined.

2 Representation of Damping

Several mathematical models have been used to represent the damping forces which arise during vibrations. For viscous damping, for single degree of freedom (SDOF), the equation for free vibrations is:

$$m\ddot{x} + c\dot{x} + kx = 0 \qquad \ldots(1)$$

In the above, m is the mass of the vibrating object, k stands for stiffness and c for the viscous damping constant. In the above, $\dot{x}$ stands for velocity and $\ddot{x}$ for acceleration. For the case of material or hysteretic damping, the experiments by Kimball and Lovell[3] and Becker and Foppl[4] led to the conclusion that this type of damping in SDOF system with simple harmonic motion of small amplitude may be treated as viscous damping with constant c for a given material may be taken as inversely proportional to frequency.

For the case of free vibrations, four models have been obtained as below:

a) $m\ddot{x} + (h/\omega)\,\dot{x} + kx = 0 \qquad \ldots(2)$

b) $m\ddot{x} + (k+ih)x = 0 \qquad \ldots(3)$

c) $m\ddot{x} + ke^{ig}x = 0 \qquad \ldots(4)$

d) $m\ddot{x} + h\,|x/\dot{x}|\,\dot{x} + kx = 0 \qquad \ldots(5)$

Kussner[5,6] has used the form (b) above for wing flutter analysis, while Myklestad[7] has represented hysteretic in the complex form (c) above. Reid's model[8] as given in (d) above, assumes that hysteretic damping is proportional to displacement but is in phase with velocity.

There has been considerable debate[9,10] on the above models. For the case of free vibrations, interpretation of ω in model (a) is not meaningful since no experiments appear to have been carried out for damped free vibration for characterisation of damping. while there is no such problem for forced harmonic vibrations. Eqs. (3) and (4) are equations with complex coefficients and the meaning is not quite clear[11,12]. Some of the salient comments regarding the above representations are:

- Use of the complex coefficients is to be avoided as done erroneously by Soroka[13] for free vibrations as it implies replacing k by $k\sqrt{1+g^2}$ where $g = h/k$
- For the case of forced harmonic vibrations, the concept of complex modulus may be used.
- A general law applicable to hysteretic damping is still to be obtained by new experiments.
- For forced vibrations of a system with hysteretic damping, the energy dissipated per cycle depends on square of the amplitude and does not depend on frequency.

Neumark[9] has proposed a tentative solution based on the dependence of energy damping due to material damping on some mean amplitude, with no dependence on frequency.

Grootenhuis[14] has compared the damping forces as in Fig. 2 for the cases of viscous, hysteretic, Couloumb and Reid models. The equations for forced vibrations are written as :

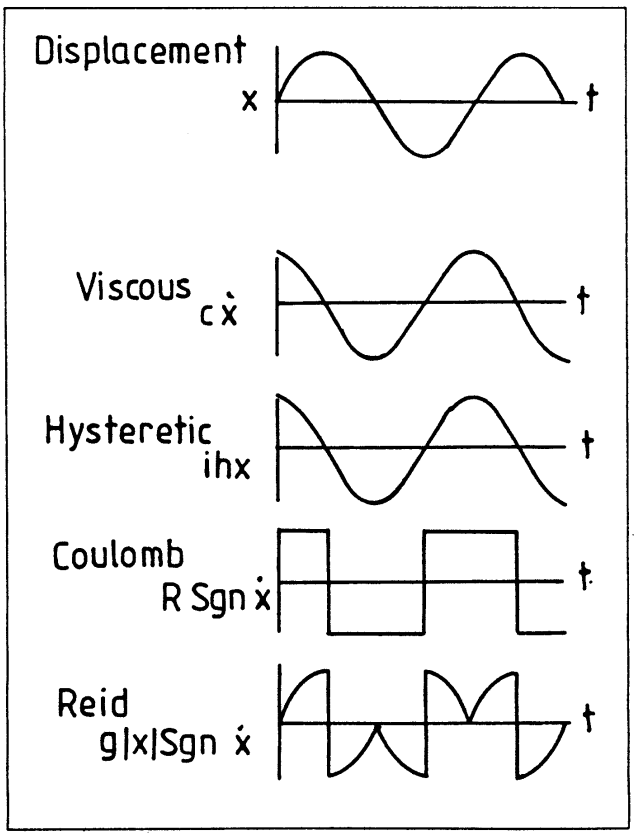

Fig. 2 Damping forces for various models[14]

$$m\ddot{x} + c\dot{x} + kx = F\,e^{i\omega t} \quad \ldots(6)$$

$$m\ddot{x} + ih\dot{x} + kx = F\,e^{i\omega t} \quad \ldots(7)$$

$$m\ddot{x} + R\,sgn\,\dot{x} + kx = F\,e^{i\omega t} \quad \ldots(8)$$

$$m\ddot{x} + g\,|\dot{x}|\,\text{sgn}\,\dot{x} + kx = \text{F}\,e^{i\omega t} \quad \ldots(9)$$

The viscous damping force is proportional to displacement and frequency, hysteretic damping force is proportional to displacement, Coulomb friction force only depends on the direction of motion and thus gives a non-linear equation of motion while Reid model is a combination of hysteretic and Coulomb damping where damping force is proportional to displacement and is independent of frequency. and may be used for both forced and free vibrations. However, further work is needed for a complete understanding of the damping process. In particular, the difficulties in describing[15] the Coulomb damping are due to its dependence on the friction which depends on the accuracy in characterising the interfaces between the surfaces and also on the environment.

The characterisation of damping in viscoelastic polymeric materials now widely used for vibration control, is done using complex moduli under harmonic excitation conditions. These moduli are seen to be dependent on frequency, temperature and strains. For transient or shock conditions, a differential operator form of representation is used to describe the stress strain relationship. The standard linear viscoelastic solid model consists of a series of derivatives related to time in the stress σ field and strain ε field[16]. It is in the form:

$$\sigma(t) + \sum_{m=1}^{M} b_m \frac{d^m \sigma(t)}{dt^m}$$

$$= E_0 \varepsilon(t) + \sum_{n=1}^{N} E_n d^n \varepsilon(t)/dt^n \quad \ldots(10)$$

A four element model in the above form has been used[17] for analysis of shock response of viscoelastically damped structures. A more refined model using fractional derivatives has been introduced[18-20] and it is shown to give a good fit to the experimental data. The general form of stress strain relation with fractional derivatives is:

$$\sigma(t) + \sum_{m=1}^{M} b_m D^{\beta_m} < \sigma(t) >$$

$$= E_0 \varepsilon(t) + \sum_{n=1}^{N} E_n D^{\alpha_n} < \varepsilon(t) > \quad \ldots(11)$$

In the above, the derivatives D are of fractional order.

There are a number of ways to measure and represent damping in materials. These include:

- Logarithmic decrement δ
- Viscous damping ratio ζ
- Loss factor η
- Q factor
- Energy ratio

Logarithmic decrement δ is derived from the free vibration decay of vibrations as in Fig. 3(a), while viscous damping ratio ζ and Q factor are obtained from the steady state response of the system to harmonic excitation as in Fig. 3 (b). As pointed out earlier, the material damping for harmonic vibrations is represented by complex modulus, the ratio of imaginary to real parts of which is called loss factor η. The relations between the above terms are as below:

$$\zeta = \delta/2\pi = \eta/2 = 1/(2Q) = D_e/(4\pi U) \quad \ldots(12)$$

where D_e is damping energy dissipated per cycle of vibration and U is the maximum strain energy in the system.

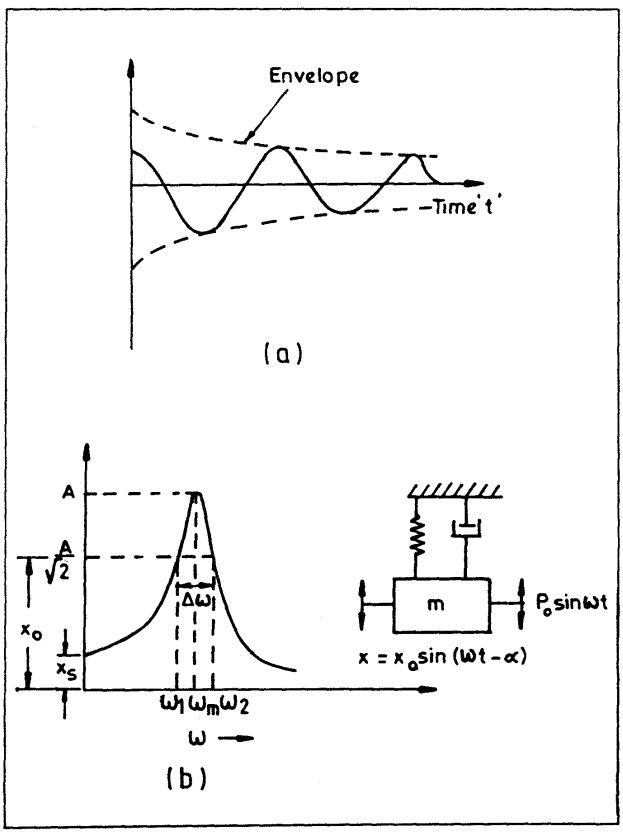

Fig. 3 Free and forced response (a) Free vibration decay (b) Steady state harmoic response

For the analysis of multi-degree freedom systems with lumped parameters or of continuous systems using finite element method (FEM), the dynamic equations of motion can be written in matrix form as below:

$$[M]\{\ddot{x}\} + [C]\{\dot{x}\} + [K]\{x\} = \{F(t)\} \quad \ldots(13)$$

where M is the mass matrix, K, the stiffness matrix and C, the viscous damping matrix. $F(t)$ is the transient excitation and x is the response. If the system has hysteretic or material damping, the above equation may be written as :

$$[M]\{\ddot{x}\} + [K + iH]\{x\} = \{F(t)\} \quad \ldots(14)$$

where H is the hysteretic damping matrix.

If damping matrix $[C]$ is a linear combination of mass and stiffness matrices as below :

$$[C] = \alpha[M] + \beta[K] \quad \ldots(15)$$

where α and β are constants, it is possible to decouple the equations of motion given in eq. (13) and the solution is easily obtainable as a linear combination of natural modes of the undamped system. This type of damping is called Rayleigh damping or proportional damping[21-23]. Similarly for Rayleigh damping of hysteretic type,

$$[H] = \alpha[M] + \beta[K] \quad \ldots(16)$$

with the above equation, it is possible to decouple eq. (14).

When it is not possible to decouple the equations for a system with non-proportional type, the eigen values and eigen vectors are complex[21-24] and the solution is quite complex.

Mohammad *et al.*[25] have discussed the role of Rayleigh damping in structures and have indicated how it may be computed based on experimental investigations.

3 Viscoelastic Damping Technology

During the past three decades, the use of viscoelastic or polymeric materials for vibration damping has acquired considerable importance due to the high value of loss factor obtainable from such materials which have the properties of both elastic and viscous elements. In such materials, the high vibratory energy dissipation is due to the disruption of the bonds of the long chain molecules in the viscoelastic materials. This technology has found several engineering applications for vibration control.

3.1 Measurement of Damping in Viscoelastic Materials

A number of experimental methods have been used to measure the damping properties of viscoelastic materials. These are reviewed in ref. [26], [27] and include log decrement free vibration decay method, use of frequency response plots near resonance and non-resonant methods. In Fig. 4, the cantilever beam method for free vibration decay of the cantilever coated with viscoelastic material is shown, in addition to the tuned damper resonant method and dynamic shear non-resonant method. The non-resonant method has the advantage that frequency and strain can be independently controlled. The method is described below and uses the set-up as in Fig. 5.

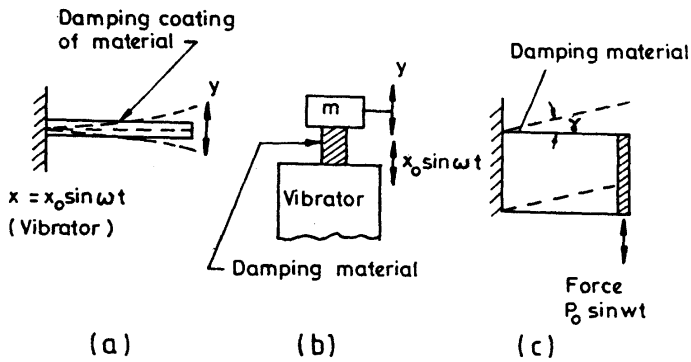

Fig. 4 Measurement of dynamic properties of damping materials (a) Coated cantilever method, (b) Tuned damper method, (c) Dynamic shear method

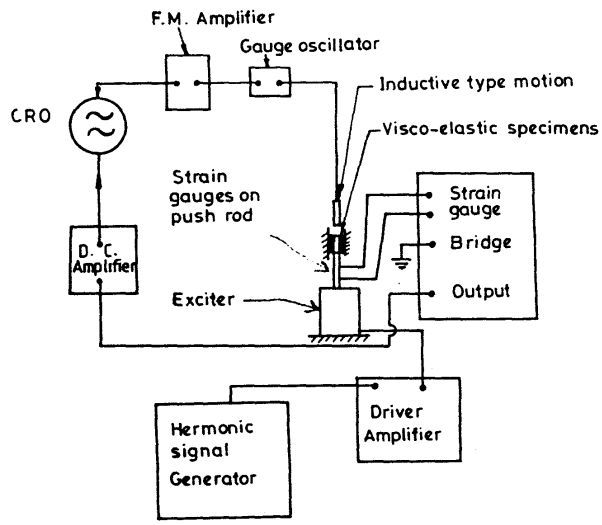

Fig. 5 Set up for dynamic shear test

If a viscoelastic material (VEM) gets strained due to harmonic stress, the strain is not in phase but lags behind by an angle θ, which is a measure of the damping in the material. The loss factor 'η' of the material equals tan θ. The ratio of stress to strain in a VEM, under harmonic excitation conditions is represented by complex moduli $E(1+i\beta)$ and $G(1+i\eta)$ in direct and shear strain respectively. These properties are seen to depend on frequency, temperature and strain. The plots of in-phase shear modulus G and loss factor η in shear for plasticized P.V.C. are shown in Fig. 6[28]. In Fig. 6(a), these are plotted against frequency for varying temperatures while in Fig. 6(b), the plots are for different values of shear strain amplitude. These were measured, in direct shear of the viscoelastic specimen with the dynamic force applied by an electro-dynamic vibrator, for varying frequencies as in Fig. 5. The shear strain amplitude was varied at different frequencies by the power amplifier of the vibrator.

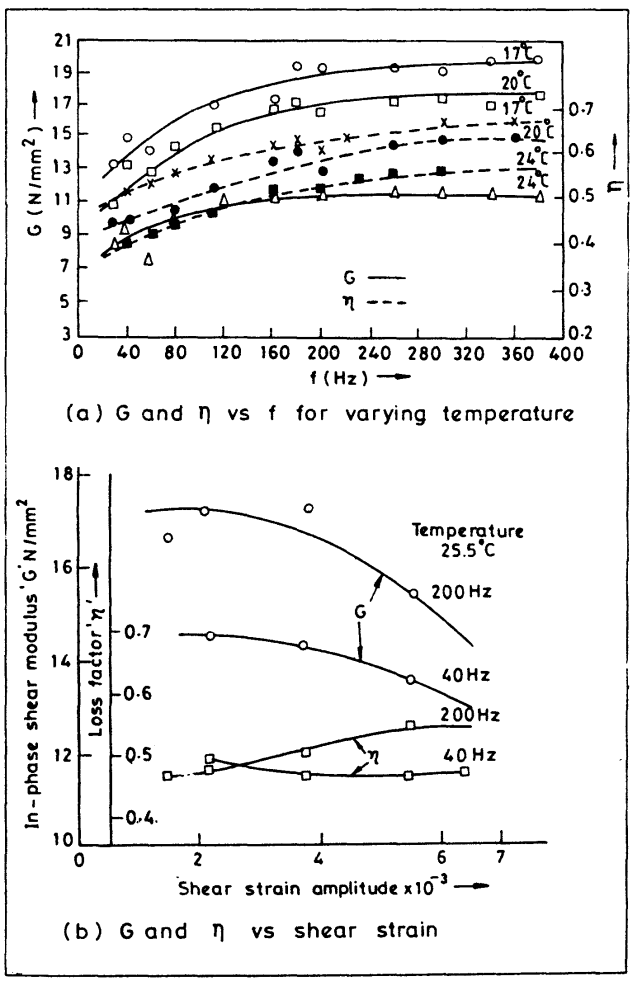

Fig. 6 Results for in-phase shear modulus 'G' and loss factor 'η' for PVC

The temperature-frequency superposition principle[29] forms the basis of reduction of the three dimensional relation between the in-phase modulus (or loss factor), frequency and temperature to a two dimensional one. This involves the use of the reduced frequency or the reduced temperature, which combines the effects of frequency and temperature by the use of factors, known as shift factors. These factors are often found empirically[27,30].

3.2 Basic Configurations Using VEM's

Some of the basic configurations used, in practice are shown in Fig. 7. The simplest arrangement is the unconstrained one in which a layer of VEM is attached to or bonded to an elastic member. The VEM may be in the form of a spray e.g. polyvinyl acetate or sheets. During flexural vibrations of the elastic member, the VEM is subjected to alternate extension and compression. In the case of constrained layer damping arrangement, the viscoelastic layer is constrained between the constraining layer and the base layer and shear strain is induced in the VEM as shown in Fig. 7 during flexural vibrations of the base layer. Another technique involves use of a tuned damper and also VEM may be used at the supports

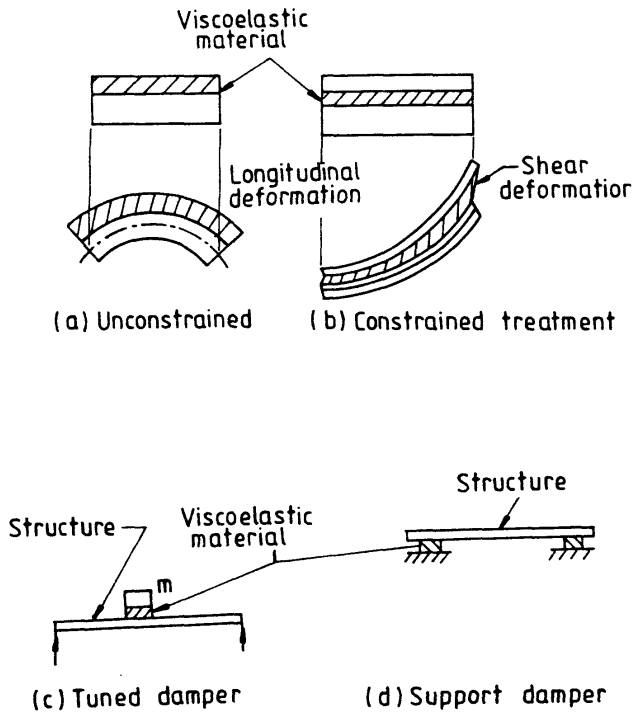

Fig. 7 Basic configurations using viscoelastic damping

of an elastic member like a shaft. Multi-layer arrangements may also be used for vibration damping.

3.3 Analysis

Analysis of structural elements like beams, plates, rings, shells or complex structures consisting of combination of such elements, involve solution of the governing equations or FEM or structural dynamic methods. The methods have been refined for computational efficiency.

For any mode 'n', the damping effectiveness of a structure, is denoted by system loss factor η_s, which is obtained from the equation:

$$[-m\omega^2 + k(1+i\eta_s)]q_n = f_n \qquad \ldots(17)$$

where f_n is the generalised excitation and q_n, the corresponding displacement while m and k are the generalised mass and stiffness respectively. A review of the work on various analysis methods, is available in ref. [31]. The system loss factor may be obtained from eq. (17).

For damping and response analysis of viscoelastically damped structural elements, the governing equations need to be formulated and solved. For harmonic excitation, the correspondence principle of viscoelasticity is used where-by the solution for viscoelastically damped cases can be obtained from that of the corresponding elastic one, by using complex moduli in place of elastic ones.

3.3.1 Constrained Layer Damping Configuration

Fig. 8 shows the constrained type beam with the assumed displacement variation across thickness. It is assumed that layers 1 and 3 bend as Bernoulli-Euler beams with $\bar{u}_1 = \bar{u}_3 = w'$, w being transverse displacement and, the differentiation with respect to x, Shear in layers 1 and 3 is ignored. w is assumed constant at a section. Only shear strains are accounted for in core 2 and the material of core 2 is assumed as linear or strain independent and no slip is assumed at the interfaces.

Shear angle γ_2 in core =

$$\bar{\alpha} - w' = \frac{u_1 - u_3}{t_2} - \frac{w'}{t_2}\left[t_2 + \frac{t_1 + t_3}{2}\right] \qquad \ldots(18)$$

where t_i is thickness of layer i (i = 1, 2, 3) and u_i is longitudinal displacement of middle of layer i(i = 1,3).

Expression for strain energy U of the beam, assuming all layers as elastic

$$= \int_0^L [s_2\gamma_2^2 + r_1 u_1'^2 + r_3 u_3'^2 + (q_1 + q_3)(w'')^2 \qquad \ldots(19)$$

where $s = \frac{1}{2} b G_2 t_2 k_2$, $q_i = \frac{b}{24} E_i t_i^3$, $r_1 = bE_1 t_1/2$, L = length, b = width, E_i = Young's modulus of layer i, G_2 = shear modulus of layer 2, k_2 = shear coefficient.

Kinetic energy T due to transverse displacements

$$= T = \int_0^L \left[\frac{\rho}{2}(\dot{w})^2\right] dx$$

Where . = Differentiation with respect to time t.

ρ = Mass per unit length

Energy V due to excitation of intensity $f(x)\sin\omega t$ is:

$$= \int_0^L f(x)\, \sin\omega t w\, dx \qquad \ldots(20)$$

Using Hamilton's principle, three governing equations and boundary conditions can be obtained[32,33].

The governing equations are as below:

$$\frac{b}{12}(E_1 t_1^3 + E_3 t_3^3)\, w^{IV} - b\, t_2\, G_2 \frac{a}{t_2}\left[w'' \frac{a}{t_2} - \frac{E_1 t_1 + E_3 t_3}{E_3 t_3}\frac{u_1'}{t_2}\right]$$

$$+ \rho\ddot{w} = f(x)\, \sin\omega t \qquad \ldots(21)$$

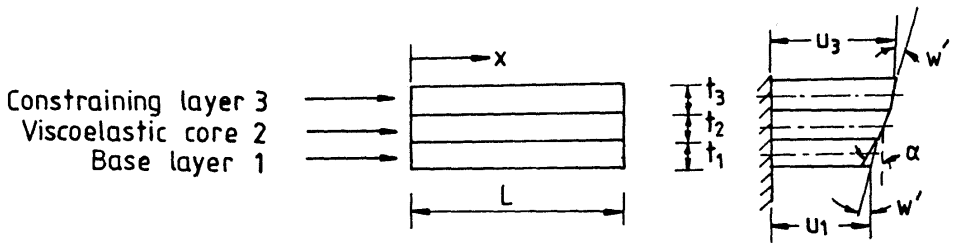

Fig. 8 Assumed displacement variations for constrained layer damping arrangements

$$b\ G_2 m'\ [\frac{w'a}{t_2} - \frac{u_1 m'}{t_2}] + \bar{D}\ u_1'' = 0 \qquad \ldots (22)$$

$$u_1 = -\frac{u_3}{m} \qquad \ldots (23)$$

where $m = \frac{E_1 t_1}{E_3 t_3}$, $m' = 1+m$, $\bar{D} = b(E_1 t_1 + E_3 t_3 m^2)$.

From the above equations, a sixth order equation in w or u_1 may be obtained which is identical to that given in refs. [34], [35]. The boundary conditions for simply supported ends are:

$$w = 0,\ u_1 = u_3 = 0.$$

The solution for simply supported ends satisfying the above end conditions is assumed as:

$$w = \sum_{n=1}^{\infty} w_n \sin\frac{n\pi x}{L} \sin\omega t \qquad \ldots (24)$$

$$u_i = \sum_{n=1}^{\infty} u_{in} \sin\frac{n\pi x}{L} \quad (i = 1,3).$$

Also $f(x)$ is written as $\sum_{n=1}^{\infty} f(x) \sin\frac{n\pi x}{L}$.

Substituting eqs. (24) in the governing equations and also using $G_2(1+i\eta_2)$ in place of G_2, we can get equations for displacements and η_s.

The expression for η_s is also identical to that by Ross *et al.*[36] and is:

$$\eta_s = \frac{H\eta_2}{(1+\alpha_{1.3}\theta_{1.3}^3)\ (M^2+\eta_2^2)\ + HM} \qquad \ldots (25)$$

where $H = \frac{3\psi_{2.3}}{\theta_{2.3}}\ (1+\theta_{1.3}+2\theta_{2.3})^2\ (1+\eta_2^2)$

$$M = \frac{\psi_{2.3}}{\theta_{2.3}}\left(\frac{1}{\alpha_{1.3}\theta_{1.3}} + 1\right)(1+\eta_2^2) + 1$$

here parameter $\psi_{2.3} = \frac{G_2}{E_3\ t_3^2\ (n\pi)^2}\ 1,\ \theta_{i.j}$

(where $\theta_{i.j} = \frac{t_i}{t_j}$ 2) and $\alpha_{i.j} = E_i/E_j$ 3, $i = 1, 2$ and $j = 3$.

A plot of η_s against $\psi_{2.3}$ as in Fig. 9 shows that η_s is maximum at a certain value of $\psi_{2.3}$ only. Thus, a change in modal number 'n' or in G_2 due to temperature or frequency change, may change the damping available.

Efforts have been made to reduce the variation by using multicored[37] as in Fig. 10 or multilayered arrangements using different viscoelastic materials.

A general analysis, applicable to any number of layers, with alternate elastic and viscoelastic layers, is reported in ref. [38] and results for system loss factor for constant weight, size and static stiffness are reported in ref. [39]. There is in general an increase

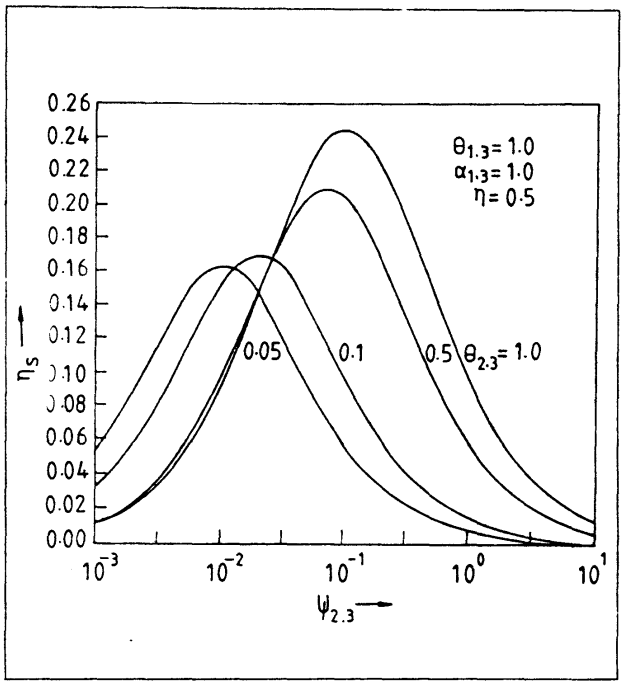

Fig. 9 A variation of system loss factor 'η_s' with shear parameter ψ 2.3

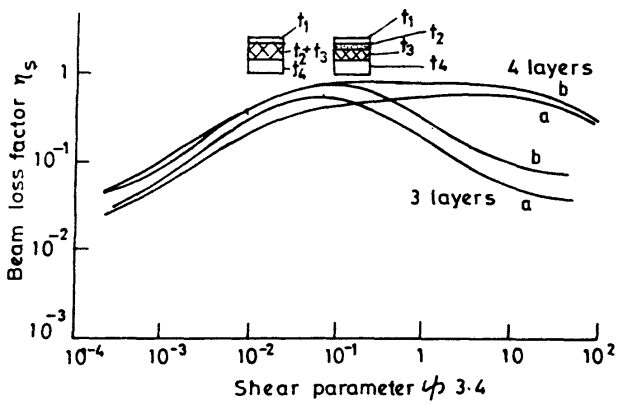

Fig. 10 Comparison of three and four layer constrained arrangements $\theta_{1.4}=\theta_{2.4}=0.5$, $\eta_2=\eta_3=1$, $\alpha_{3.4}=0.01$, $\alpha_{1.4}=0.33$, $G_3/G_2=1000$ Curves *a* : $\theta_{2.3}=2.5$, Curves *b* : $\theta_{3.4}=5$

in maximum system loss factor with an increase in the number of layers.

Mead[40] carried out a detailed comparison of the equations for flexural vibrations of the equations of damped sandwich beams. A sixth order equation in transverse displacement 'w' is obtained from ref. [34,35] which is similar to that obtained from eq. (21) to (23). However, Yan and Dowell[41] obtained a fourth order equation in 'w' for the same problem. The difference was attributed to the fact that in ref. [41], an assumption of uniform shear stress through the depth of the whole sandwich was made, which is not strictly applicable especially for a soft and thin core. The solution of governing equations for damped sandwich beams for various boundary conditions is given in refs. [42],[43]. In ref. [44], an approximate solution for finding forced response to harmonic excitation is given for fixed-fixed and cantilever type boundary conditions, using Rayleigh-Ritz method and correspondence principle of viscoelasticity.

3.3.2 Unconstrained Layer Damping Arrangement

The arrangement is shown in Fig. 11 and uses a viscoelastic layer bonded to an elastic beam. If u_1 and u_2 are extensions of the middle of layers 1 and 2 respectively and w is the transverse displacement at a section, with w' as the slope at a section,

$$u_2 = u_1 - w'(t_1 + t_2)/2 \qquad \ldots (26)$$

Total strain energy U for the beam of length L is equal to:

$$bE_1t_1^3/24\int_0^L (w'')^2dx + bE_2t_2^3/24\int_0^L (w'')^2dx$$

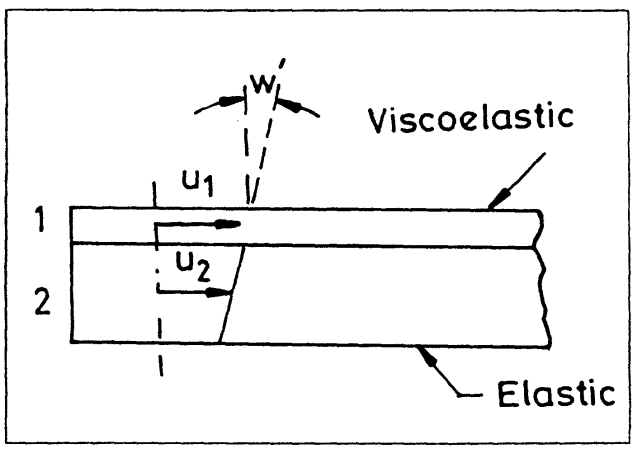

Fig. 11 Assumed displacement variations for unconstrained damping arrangements

$$+bE_1t_1/2\int_0^L (u_1')^2dx + bE_2t_2/2\int_0^L (u_2')^2dx \qquad \ldots(27)$$

Kinetic energy $T = {}^1/_2\ \rho \int_0^L (\dot{w})^2\ dx$ $\qquad \ldots(28)$

where ρ is mass/unit length $= b(\rho_1t_1 + \rho_2t_2)$, with ρ_1 and ρ_2 being the mass densities of layers 1 and 2 respectively.

Energy of external force $V = \int_0^L wf(x)\sin\omega t\,dx, \ldots(29)$

Substituting eq. (26) in eq. (27), taking $u_1 = u$ and carrying out variations in w and u in eq. (27) to (29) and applying Hamilton's principle, we get the equations of flexural vibrations as below:

$$fu'' - gw'' = 0 \qquad \ldots(30)$$

$$kw^{iv} - gu''' + \rho\ddot{w} = f(x)\ \sin\omega t \qquad \ldots(31)$$

where $k = b[E_1t_1^3/12 + E_2t_2^3/12 + E_2t_2(t_1/2 + t_2/2)^2]$

$f = b(E_1t_1 + E_2t_2)$

$g = b\ E_2t_2\ ((t_1 + t_2)/2)$.

The boundary conditions for simply supported ends viz. $x = 0$ and $x = L$ are:

$w = w'' = u' = 0$. These are satisfied by equations similar to eq. (24) and substitution of the same in eqs. (30) and (31) gives

$$w_n = \frac{f_n}{(n\pi/L)^2(k - g^2/f) - \rho\omega^2} \qquad \ldots(32).$$

For the viscoelastic layer, substituting E_1 by complex modulus $E_1(1+i\eta)$, with E_1 as the inphase modulus and as the material loss factor, in the same way as for the constrained layer damping arrangement as below:

$$\eta_s = \frac{\eta h_1 e_1(3 + 6h_1 + 4h_1^2)}{1 + e_1h_1(3 + 6h_1 + 4h_1^2)} \qquad \ldots(33)$$

where $h_1 = t_1/t_2$ and $e_1 = E_1/E_2$.

In the above, the following have been assumed.

$e_1\ h_1 << 1$ and $\eta E_1t_1 << E_2t_2$

A plot of η_s/η is given in Fig. 12. It is seen that

η_s/η increases with increase of h_1 and e_1 in general. The results are identical to those given by Oberst[45].

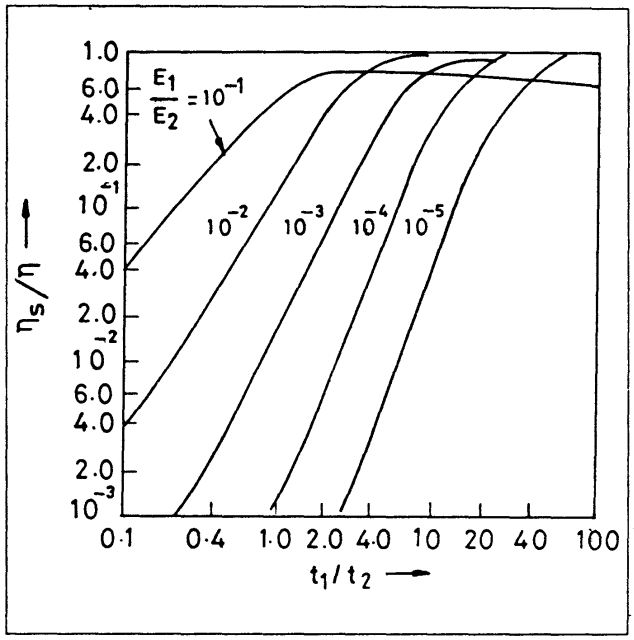

Fig. 12 Variation of system damping with thickness ratio of unconstrained layer damping arrangement

3.3.3 Rotor System on Viscoelastic Supports

Viscoelastic damping at the supports of rotating systems can be quite effective in controlling the response and stability of the system.

Fig. 13 shows a Jeffcott rotor with ball bearings at each end, with viscoelastic supports. M_2 is the mass of the disc symmetrically located at the middle of the shaft with K_b representing the total bearing stiffness, C_b is the total bearing damping constant. M_1 is the total bearing support mass and K^* is the

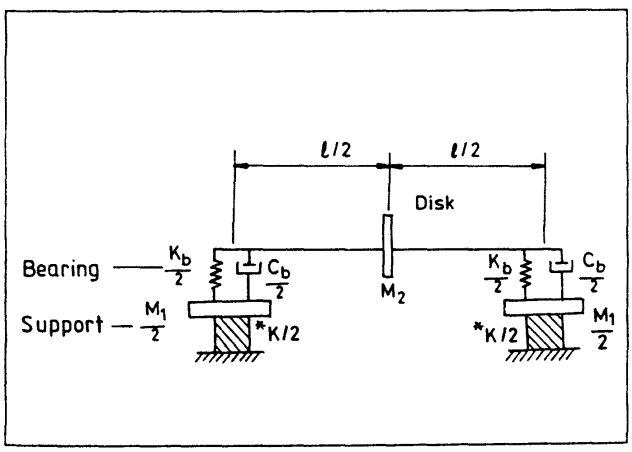

Fig. 13 Schematic diagram of rotor in bearings on viscoelastic supports

total stiffness of the supports. The equations of motion can be written as:

$$M_2\ddot{z}_2 + K_s z_s = M_2 e_u \omega^2 e^{i\omega t} \quad \ldots(34)$$

$$K_b z_j + C_b \dot{z}_j - K_s z_s = 0 \quad \ldots(35)$$

$$M_1\ddot{z}_1 + K^* z_1 - K_s z_s = 0 \quad \ldots(36)$$

In the above, z_2 is the displacement of the rotor disc, z_j that of the journal relative to the support, z_l is support displacement, ω is the rotational angular speed and z_s is the displacement of the shaft at the rotor location, relative to the ends of the shaft. For harmonic excitation, $K^* = K(1+i\eta)$, where K is the in-phase stiffness of the supports and η is the loss factor of the viscoelastic material at the supports. Further, e_u is the eccentricity of the rotor disc mass.1

Assuming the solution as :

$$z_2 = Z_2 e^{i\omega t}, z_j = Z_j e^{i\omega t}, z_1 = Z_1 e^{i\omega t} \quad \ldots(37)$$

where Z_2, Z_j, Z_1 are complex. Further,

$$z_s = z_2 - z_j - z_1 \quad \ldots(38)$$

Substituting eqs. (37) and (38) in eqs. (34) to (36) and non-dimensionalizing, we get

$$(1-\delta^2)z_2 - z_j - z_1 = e_u\delta^2 \quad \ldots(39)$$

$$z_2 - [(1+\beta) + i2\varsigma\delta]z_j - z_1 = 0 \quad \ldots(40)$$

$$z_2 - z_j - [(1-\alpha\delta^2 + \beta_1) + i\beta_1\eta]z_i = 0 \quad \ldots(41)$$

where α =mass ratio =M_1/M_2

$\beta = K_b/K_s$, the bearing stiffness ratio,

$\delta = \omega/\omega_n$, ω_n being the circular natural frequency of the system if supported on rigid supports $= \sqrt{K_s/M_2}$, $\varsigma = C_b/C_c$, where C_c is the critical damping constant $= 2M_2\omega_n$.

The above equation can be used to find the rotor amplitude ratio $R_D = |Z_2|/e_u$. Fig. 14 shows a plot of R_D against δ_R for the chosen parameters giving two peaks. Fig. 15 shows the peak values of R_D viz. R_{D1} and R_{D2} and the corresponding frequencies δ_{R1} and δ_{R2} respectively for varying values of β_1. It is seen that an optimum value of β_1 is necessary for limiting both the peak amplitude ratios and the same may correspond to the point of intersection of R_{D1} and R_{D2} curves. The characteristics of viscoelastic materials are assumed to be frequency independent in the above analysis.

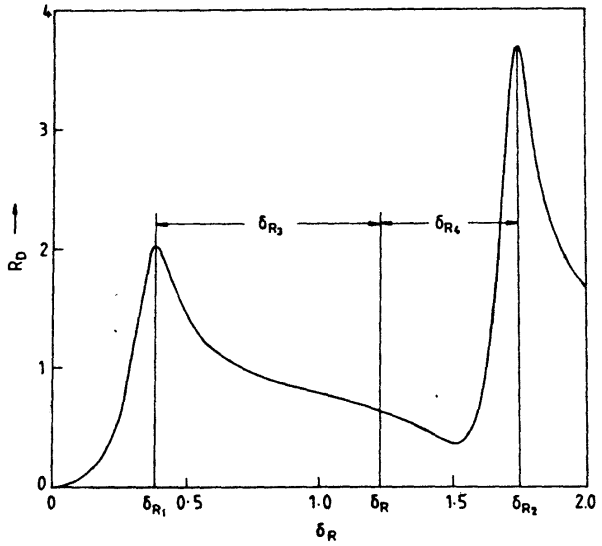

Fig. 14 Typical unbalance response amplitude of the rotor with linear elastic bearings at the ends with viscoelastic supports α=0.4, β=3.0, β_1=0.2, η=0.5

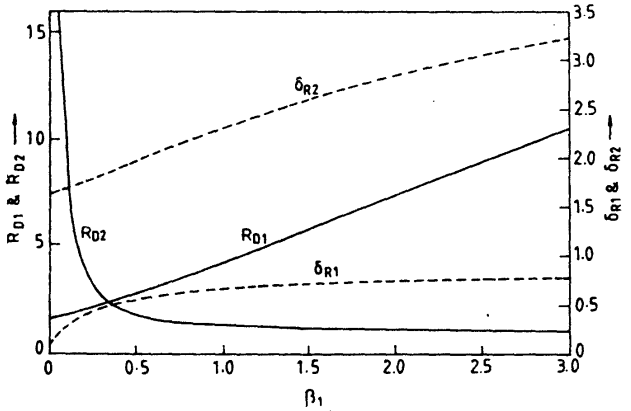

Fig. 15 Variation of peak response values and corresponding frequencies with support stiffness parameter β_1
- First peak response (R_{D1}), - Second peak response (R_{D2})
--- First peak frequency (δ_{R1}), --- Second peak frequency (δ_{R1})

In order to reduce the amplitude ratio of vibrations, an algorithm has been tried in ref. [46] to determine the desired dependence of viscoelastic material properties on frequencies. The algorithm is based on the location of the two resonance frequencies δ_{R1} and δ_{R2} as in Fig. 14. For each value of δ_R, values of β_1 and η are tried so that δ_{R3} and δ_{R4} are $\geq c$, the comparison constant which is suitably chosen so that the two resonant frequencies are located as above. The other possibilities viz.

i) $\delta_{R3} < c$ and $\delta_{R4} > c$

ii) $\delta_{R3} > c$ and $\delta_{R4} < c$

iii) $\delta_{R3} < c$ and $\delta_{R4} < c$

are discarded. The unbalance response of a frequency-dependent VEM, (with characteristics as in Fig. 17 is seen to be lower than that of a frequency-independent VEM at the supports, as shown in Fig. 16. Depending on the initially chosen values of β_1 and η, different desired characteristics of the support, may be obtained.

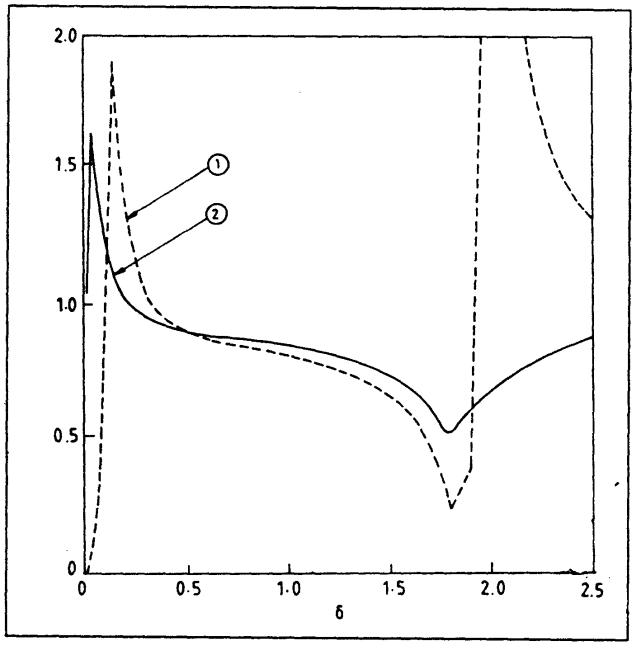

Fig. 16 Unbalance response amplitude, α=0.42, β=2.0, β_1=0.02, η=0.5, ζ=0,
--- (1) Frequency independent support characteristics
- (2) Frequency dependent support characteristics

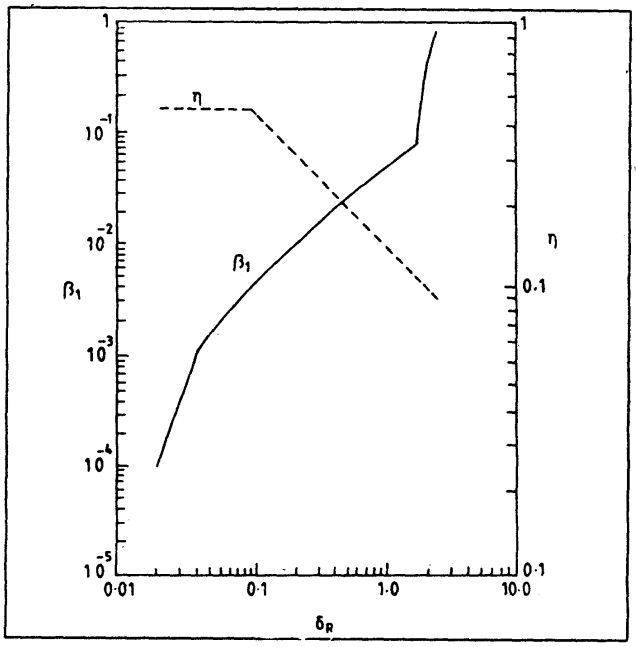

Fig. 17 Viscoelastic material characteristics for frequency dependent supports

It has also been shown in refs. [47],[48] that the stability limit of the rotor-shaft system in the case of material damping of the system or due to hydrodynamic bearings at the ends, can be improved by using suitable viscoelastic support parameters. The stability analysis has been carried out by using a four element type of model of the viscoelastic material as in Fig. 18, for which the equivalent stiffness K_{eq}. is given by

$$K_{eq} = (\gamma + \gamma_1 D + \gamma_2 D^2)/ (1+ \alpha_1 D) \quad ...(42)$$

Where $\gamma = K_1$, $\gamma_1 = \eta_2 + \eta_3 + K_1\eta_3 /K_3$, $\gamma_2 = \eta_2\eta_3 /K_3$, $\alpha_1 = \eta_3 K_3$ and D stands for d/dt.

For the case of hydrodynamic bearings at the two ends and viscoelastic supports, the configuration models in x-z and y-z planes are shown in Fig. 19. The equations of motion of the system are[48]:

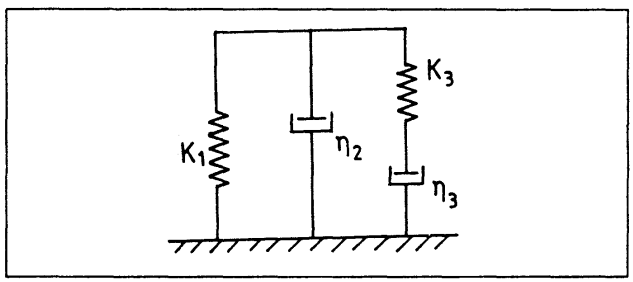

Fig. 18 The four element viscoelastic model

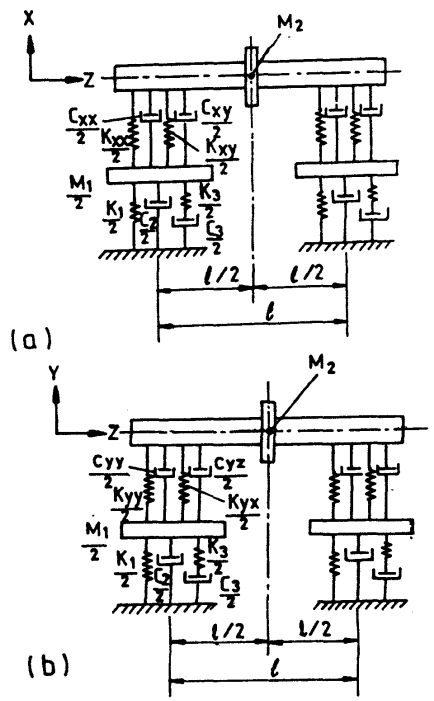

Fig. 19 Configuration model in (a) x-z plane, (b) y-z plane

$$M_2\ddot{x}_2 + K_s x_s = 0 \quad ...(43)$$

$$K_{xx}x_j + K_{xy}y_j + C_{xx}\dot{x}_j + C_{xy}\dot{y}_j - K_s x_s = 0 \quad ...(44)$$

$$M_1\ddot{x}_1 + k_{eq}x_1 - K_s x_s = 0 \quad ...(45)$$

$$M_2\ddot{y}_2 + K_s y_s = 0 \quad ...(46)$$

$$K_{yy}y_j + K_{yx}x_j + C_{yy}\dot{y}_j + C_{yx}\dot{x}_j - K_s y_s = 0 \quad ...(47)$$

$$M_1\ddot{y}_1 + k_{eq}y_1 - K_s y_s = 0 \quad ...(48)$$

where K_{xx}, K_{yy} are the stiffnesses and C_{xx} and C_{yy} are the damping coefficients of the journal bearings, K_{xy} and k_{yx} are the cross-coupled stiffnesses, C_{xy} and C_{yx} are the cross-coupled damping coefficients for the journal bearings. The expression for K_{eq} is used as in eq. (42) and x_s and y_s are substituted in eqs. (43) to (48) as below:

$x_s = x_2 - x_j - x_1$ and $y_s = y_2 - y_j - y_1$.

Using $x_n = X_n e^{rt}$, $y_n = Y_n e^{rt}$ (for n = 1,2)

$x_j = X_j e^{rt}$ and $y_j = Y_j e^{rt}$,

the 12th order characteristic equation is obtained from which the roots of the polynomial are obtained using Bairstow's method. Stability limit of the rotor speed for the system are obtained from the nature of the roots. If the real part of any root is positive, it signifies instability of the system.

The data of the rotor-shaft system for which the stability analysis is done, is given below.

Mass of the rotor=220 Kg., Shaft length=0.544 m, EI of the shaft=1.0784 Nm^2

Diameter of the journal bearing=10.16 cm., Bearing length=5.08 cm.

Bearing radial clearance=10.16×10^{-3} cm.

Oil viscosity=5.68×10^{-3} NS/m^2

The expressions for various direct and cross coupled stiffness and damping coefficients of the journal bearings in terms of the Sommerfeld Number have been given in ref. [49] and the values have been determined accordingly.

Further, Support mass ratio α = 0.1, Primary support stiffness ratio = β_6 = 0.1

Secondary support stiffness ratio = β_7 = 0.2, Primary damping ratio = ζ_5 = 0.01,

Secondary damping ratio = ζ_6 = 0.1.

Fig. 20 shows the plot of real part of the roots of the characteristic equation as the speed of the rotor is varied from 2000 to 20,000 rpm for different values

of β_6.The positive real part of a root signifies instability while the negative real part of the root signifies stability. It is found that for low values of β_6, the system is stable throughout the speed range of the rotor while for higher values of β_6, the stability limit falls sharply and for the rigid support condition, i.e. for high values of β_6, the system is stable only upto a speed of 5400 rpm of the rotor, after which the system becomes unstable.

Fig. 21 shows the stability of the system drawn against changing values of β_6. It shows that for having a wide stability limit, the value of β_6 should be as low as possible.

Thus the use of a suitable VEM at the support increases the stability limit of the system. It has also been shown in ref. [47] that the stability zones for the case of internal damping in the rotor can be enhanced by using suitable supports made of VEMs.

3.4 Structural Dynamic Modification and Optimum Design

In view of the large number of parameters, dynamic optimum design using damping is carried out usingSDM (Structural Dynamic Modification) and multi-parameter optimisation.

3.4.1 Structural Dynamic Modification

For studying the influence of various damping additions to an untreated structure, perturbation techniques are used, treating modification as a small perturbation to the original structure[50]. With the above, it is possible to estimate the eigen properties of the modified system by expressing the increments in eigen parameters in terms of increments in stiffness and mass matrices of the system during modification.

The perturbation equations for the changes in eigenvalue, $\Delta\lambda$ and in eigenvector$\{\Delta\psi\}$ for given changes in stiffness and mass matrices[50-52] are:

$$\Delta\lambda_i \approx \frac{\{\psi_i\}^T[\Delta K - \lambda_i \Delta M]\{\psi\}_i}{\{\psi_i\}^T[M]\{\psi\}_i} \qquad \ldots(49)$$

and $\{\Delta\psi\}_i \approx \Sigma p_{ij}\{\psi\}j,\ i \neq j$

where, $P\lambda_{ij} \approx \dfrac{\{\psi_i\}_j^T[\Delta K - \lambda_i \Delta M]\{\psi\}_i}{(\lambda_i - \lambda_j)\{\psi\}_i^T[M]\{\psi\}_i}$

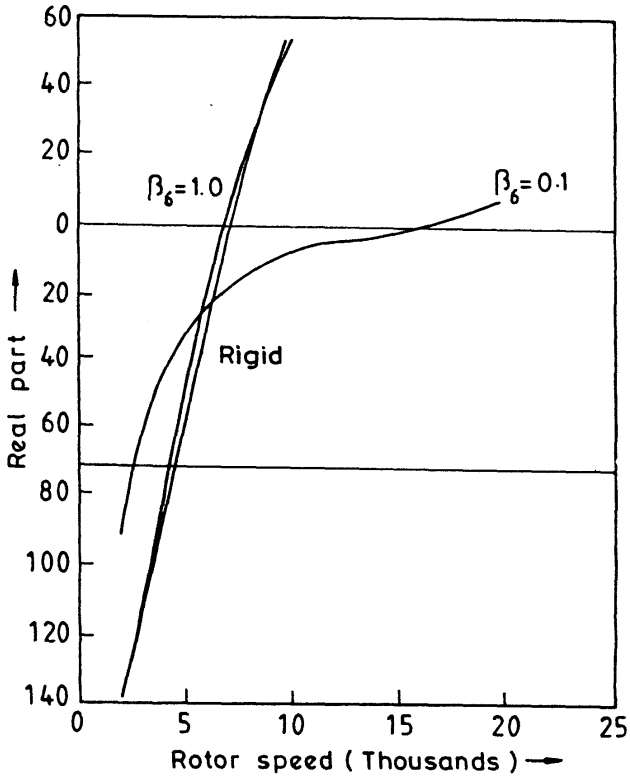

Fig. 20Real part of the root of characteristic equation vs. rotor speed α=0.1, β_7=0.2, ζ_5=0.01, ζ_6=0.1

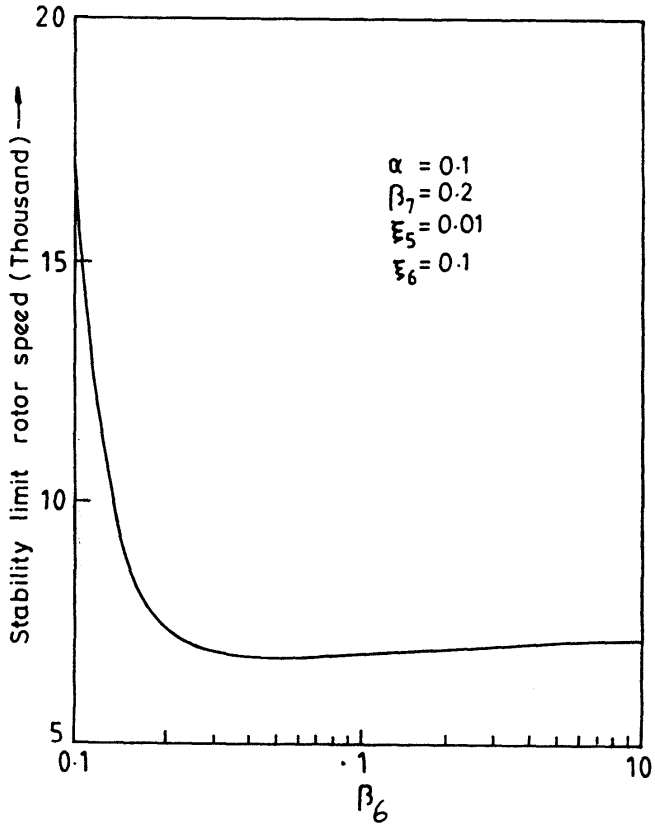

Fig. 21 Effect of β_6 on stability

For obtaining the matrices of the original and modified systems, FEM has been used and for finding the damped natural frequencies and system loss factor, a standard eigen value solver is used. Modal summation is then used to find the response to excitation.

The eigenvalue problem may be stated as under:

$$\lambda_i[M]\{\psi\}_i = [K]\{\psi\}_i \qquad \ldots(50)$$

For a system with modification,

$$\lambda_i = \lambda_i + \Delta\lambda_i \qquad \ldots(51)$$

and $\{\psi\}_i = \{\psi\}_i + \{\Delta\psi\}_i$

where $\lambda_i = \omega_i^2 (1 + i\eta_i)$ ...(52)

λ_i is the eigenvalue of the ith mode and $\{\psi\}_i$ is the corresponding mode shape, ω_i is damped natural frequency and η_i is modal loss factor of the system.

The steps for structural dynamic modification or reanalysis are :

1. Solve eigenvalue problem viz. eq. (50) for the original system.
2. Find $[\Delta M]$ and $[\Delta K]$ for the modifications. If these are large, divide into smaller ones.
3. Solve equations for $\Delta\lambda_i$ and $\{\Delta\psi\}_i$ for changes $[\Delta M]$ and$[\Delta K]$ using equations given in eq. (49)
4. Update the modal parameters using eq. (51).
5. Repeat steps 2-4 till the desired modifications are got.
6. Solve for w_i and η_i using eq. (52).

Using the above method, the results of a partially covered F structure for various constrained type coverages are given in Fig. 22. The data used is given in ref. [51]: $b = t_1 = 0.05$ m, $t_2 = t_3 = 0.025$ m. The base and constraining layers are of mild steel while the core layer has Young's modulus equal to 1/100th of that of the base layer, density 1/5th of the base layer density and material loss factor of 0.6. The results using the above SDM method based on perturbation, are seen to be in agreement with those obtained by re-solution using FEM. Also, the influence of locations of coverages from 1 to 4 may be seen on the damping effectiveness of the system.

Fig. 23 gives similar results for resonant frequencies and amplitude ratio for a partially covered fixed-fixed beam for the first two modes[52]. The results by both the methods viz. perturbation and re-solution are in agreement. The data used is: L = 1.0m, t_1 = 0.01m, $t_2 = t_3$ = 0.005 m, $E_3 = E_1 = 7 \times 10^{10}$

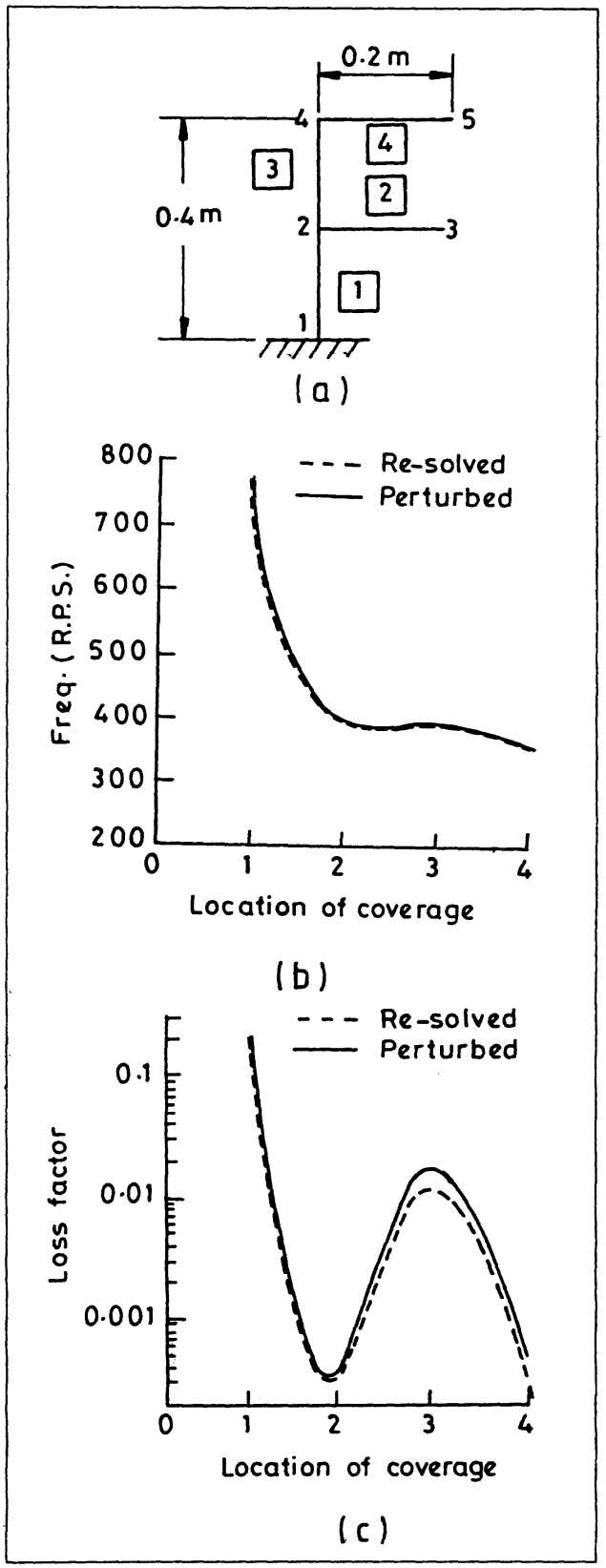

Fig.22 The F structure and the effect of constrained damping coverage location

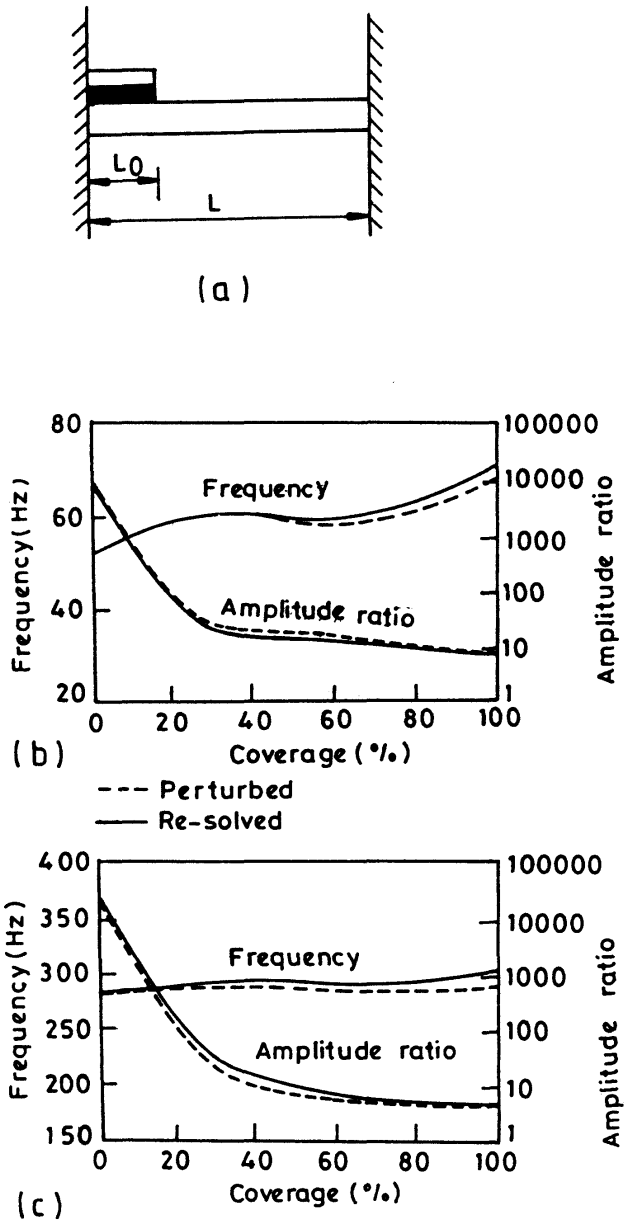

Fig. 23 Resonance characteristics of beams with partial coverage

N/m^2, $G_2 = 1.962 \times 10^7$ N/m^2, $\eta^2 = 0.4$. Mass densities $\rho_1 = \rho_3 = 2700$ Kg/m^3, $\rho_2 = \frac{\rho_1}{2}$. It is seen that in both the cases, perturbation method is very efficient computationally and may be applied to complex structures.

3.4.2 Optimum Dynamic Design using Multi-Parameter Optimisation

Multi-parameter optimisation studies are useful since the number of parameters in systems incorporating viscoelastic damping is large.

Optimum design studies for a sandwich plate with partially covered constrained damping treatment, have been carried out in refs. [53],[54]. Rayleigh-Ritz method has been used for simply supported rectangular plate. Table I gives results for additive damping at locations 1,3 and 13 on the plate shown in Fig. 24. The results are compared with these of a fully covered plate for the same total mass[53]. F.C. refers to the fully covered plate and PCL-1 refers to partially covered location 1. This also applies to PCL-3 and 13. For the base plate, $L = W = 0.4$m, thickness = 0.005m. For the VEM, in-phase shear modulus = 4×10^6 N/m^2, loss factor = 0.38 and $m = n = 1$. Young's modulus of the base and constraining layer equal 2.07×10^{11} N/m^2 and Poisson's ratio = 0.334. $\eta_{m,n}$ was chosen as the system loss factor for m,n^{th}. mode to be maximized, with design parameters as P_L, P_w, t_2 and t_3, with the patch coverage area limited to 40% of the base plate area. The added mass of

Table I

Comparison of results with optimum values of parameters for fully and partially covered plates

Values	FC	PCL-1	PCL-13	PCL-3
ω_{mn}	940.6	897.3	897.1	923.7
η_{mn}	0.048	0.024	0.043	0.054
P_L (m)	0.4	0.24	0.19	0.16
P_W (m)	0.4	0.3	0.35	0.38
t_3 (m)	0.5×10^{-3}	0.23×10^{-2}	0.26×10^{-3}	0.28×10^{-2}
t_2 (m)	0.25×10^{-2}	0.12×10^{-2}	0.72×10^{-3}	0.5×10^{-2}

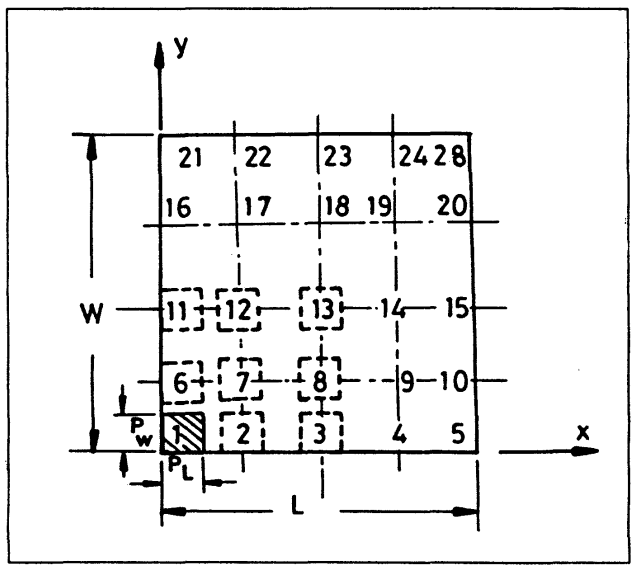

Fig. 24 Plate with damped patches

the patch was equal to that for the fully covered case. It is seen from Table I that higher system loss factor $\eta_{m,n}$ may be obtained by partial coverage at a suitable location compared to that for a fully covered case.

The algorithm used involved a constrained search strategy[55] in which a constrained problem is made an unconstrained type by application of external parabolic penalty functions. The n-dimensional space is first randomly scanned for limited number of points and the minimum value is taken as the starting base points. Sequential interval halving is used to find the minimum along the steepest direction. The search is continued till the accuracies on the design variables and the objective function, are met.

Another optimisation problem involves maximizing the system loss factor $\eta_{m,n}$ by varying the dimensions of the rectangular patch for the three locations[53]. Area of the patch equals that of a square patch with $P_L = P_W = 0.15$ m. The data is same as for previous study with the thickness of viscoelastic layer = 0.0025 m and that of the constrained layer = 0.0005 m. Table II shows the optimised dimensions of the rectangular patch and the corresponding values of $\eta_{m,n}$ which would be higher than that of a square patch at the same location for PCL-3 and PCL-13. In the above, $m = n = 1$.

Table II

Comparison of results with square and optimum rectangular patches with same covered area

Values	PCL-1		PCL-13		PCL-3	
	Square	Opt. Rect.	Square	Opt. Rect.	Square	Opt. Rect.
ω_{mn}	968.1	973.4	930.8	952.1	955.7	952.0
η_{mn}	0.184×10^{-2}	0.19×10^{-2}	0.3×10^{-2}	0.77×10^{-2}	0.11×10^{-2}	0.77×10^{-2}
P_L(m)	0.15	0.06	0.15	0.39	0.15	0.06
P_W(m)	0.15	0.39	0.15	0.06	0.15	0.39

In refs. [56], [57], work on the multi-parameter optimisation of viscoelastically damped structural elements is reported using various optimisation strategies. Work on the optimum dynamic design using SDM and optimisation using sensitivity analysis is also reported in refs. [58], [59].

3.5 Applications

A number of applications of viscoelastic damping technology are reported in refs. [27, 31, 60, 61]. These include instrument panels of aero-space systems, radar antennas, inlet guide vanes of jet engines, crankcase and cylinder walls of engines, buildings and bridges, ship structures, machine tools, automotive vehicle body, transmission covers, electrical home appliances etc. The damped laminates are commercially available. The vibration and noise control measures using damping can thus be incorporated at design stage rather than as after thoughts.

4 Active Damping

Currently, research work is being actively pursued for using active damping of vibrations by sensing vibrations and after suitable signal processing feeding the electrical signal to actuators which apply control forces on the vibrating structures for controlling the structural vibrations. Fig. 25 shows a feed back system using an electrodynamic sensor as a discrete actuator, receiving its input signal from the sensor after processing. Distributed type of piezoelectric coated sensors and actuators as in Fig. 26 are also used for controlling a number of modes of the flexible structures as in aero-space and robotic applications.

Some of the other recent developments involve the use of intelligent treatments whose damping characteristics can change, in response to the applied voltage. Fig. 27 shows an arrangement using electro-rheological (ER) materials which is currently being explored. Stiffness and damping properties of ER materials can be controlled by voltage '*V*' applied through feedback devices. The structures of this type are called ultra-advanced intelligent composite materials[62].

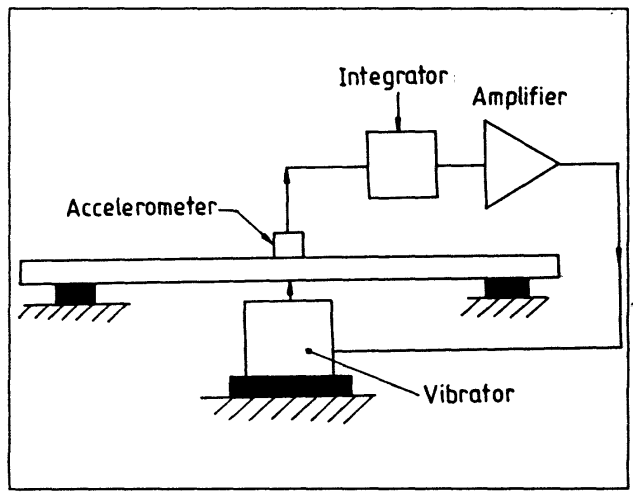

Fig. 25 Activedamping using concentrated electrodynamic vibrator

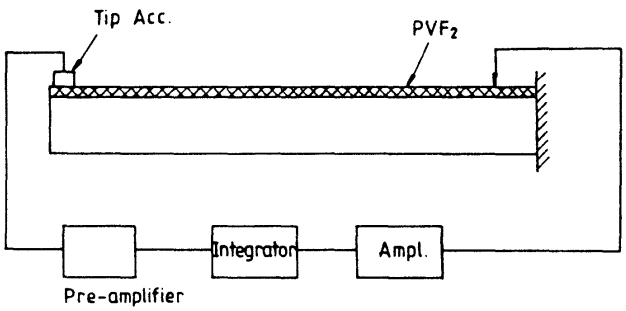

Fig. 26 Active damping using distributed PVF_2 damper

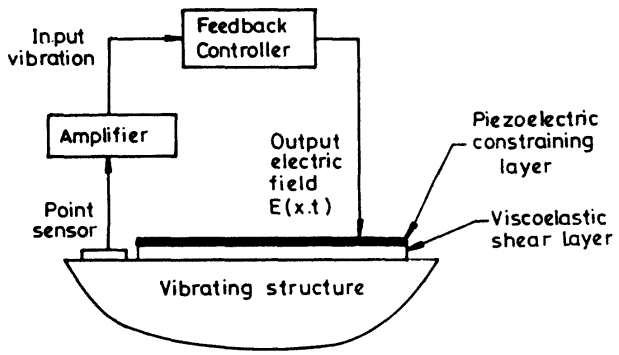

Fig. 27 Intelligent damping treatment using ER fluid

Another novel arrangement[63] uses active piezoelectric layers on both sides of a viscoelastic core which are attached to the base layer. One of the active layer acts as a sensor, whose output after amplification, is applied to the active constrained layer, giving added damping due to increased shear strain in the core. Such damping treatments are called intelligent constrained layer (ICL) or active constrained layer (ACL) treatments in which costrained layer damping and active feedback control are integrated. Shen[64] has recently studied the control characteristics of such an arrangement.

5 Emerging Trends and Future Work

After the classical book by Lazan[1] on damping of materials and members, a few books have appeared of late on the subject[27,65,66,67,68] due to the increased interest in the subject in the last few years. Recently, Jones[69] has given his reflections on the damping technology at the end of this century expecting damping applications to continue in the next century in view of the fact that vibrations and noise are here to stay. This is also reflected in the report by Singh and Nakra[70] on the Indo-US symposium on the "Emerging Trends in Vibrations and Noise Engineering" recently held in New Delhi.

Some of the emerging trends and future work is expected on the following lines[71].

a) There would be greater emphasis on built-in damping at design stage rather than providing it as an after thought, thus treating damping as a design parameter[72].

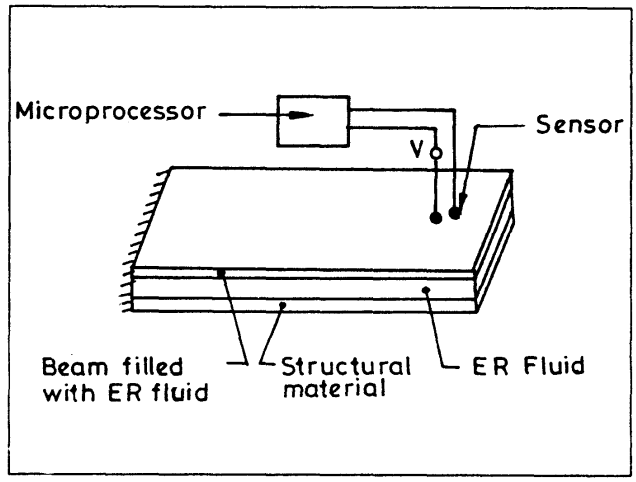

Fig. 28 Active constrained layer damping treatment

b) Keeping in view the reliability and economic considerations, a combination of passive damping and active devices for continuous flexible systems, may be used.

c) Further attention may be devoted to analysis for refinement of theories to incorporate non-linear viscoelastic models, shock and random excitations, development of approximate closed form solutions for structural elements with additive viscoelastic damping and analysis of machinery isolation systems incorporating high damping VEMs.

d) Work on development of viscoelastic materials, with less variation of dynamic properties, over a wide range of temperatures and frequencies, in addition to work on development of intelligent materials giving desired dynamic stiffness and damping over prescribed frequency and temperature ranges and analysis of structures with the above, is likely to be emphasised.

e) Optimisation studies of dynamic response, covering a large frequency range over a number of modes, need to be carried out. Dynamic optimum design studies on complex systems involving sensitivity analysis and re-analysis, should also be of interest.

f) Analytical evaluation of reduction in noise radiation from structures with additive damping and exposed to dynamic environment, does not appear to have been carried out and should be of interest.

References

1 B J Lazan *Damping of Materials and Members in Structural Mechanics* Pergamon Press (1968)

2 J E Ruzicka (Ed.) *Structural Damping* ASME Publ. (1960)

3 A L Kimball and D E Lovell *Physical Review* **30** (1927)

4 E Becker and O Foppl *Forschungsh Ver Dtsch* Ing No 304 (1928)

5 H G Kussner *DVL-Jahrbuch* (1929) 313

6 H G Kussner *Luftfahrtforsch* **12** (1935) 193

7 N O Myklestad *J Appl Mech* **19** (1952) 284

8 T J Reid *J Royal Aero Soc* **60** (1956) 283

9 S Neumark *Aero Res Council R & M* No 3269 HMSO London (1962)

10 C W Bert *J Sound Vibn* **29** (1973) 129

11 P Lancaster *J Royal Aero Soc* **64** (1960) 229

12 R D Milne *Symp Structural Dynamics* Loughborough Univ of Tech, UK (1970)

13 W W Soroka *J Aero Sci* **16** (1949) 409

14 P Grootenhuis *Control of Noise and Vibration Environment* Inaugural Lecture, Imperial College of Sci and Tech Univ of London (1974)

15 A V Srinivasan *Proc Damping'84* California USA (1984) I-1

16 D R Bland *The Theory of Linear Viscoelasticity* Pergamon Press, Oxford (1960)

17 A D Kapur, B C Nakra and D R Chawla *J Sound Vibn* **55** (1977) 351

18 R L Bagley and P J Torvik *AIAA Jour* **21** (1983) 741

19 L Rogers *J Rheology* **27** (1983) 351

20 R L Bagley and P J Torvik *Amer Inst Aero & Astr J* **23** (1985) 918

21 S S Rao *Mechanical Vibrations* Addison–Wesley Publ (1995)

22 N M M Mai *et al. Theoretical and Experimental Modal Analysis* John Wiley Publ (1997)

23 D J Inman *Vibrations with Control, Measurement and Stability* Prentice Hall New Jersey (1989)

24 L D Mitchell *Proc 8th IMAC* (1990) 891

25 D R A Mohammad, N V Khan and V Ramamurti *J Sound Vib* **185** (1995) 207

26 S O Oyadiji and G R Tomlinson *J Sound Vibn* **101** (1985) 277

27 A D Nashif D I G Jones and J P Henderson *Vibration Damping* John Wiley New York (1985)

28 N T Asnani *Vibration Analysis of Multilayer Beams with Constrained Viscoelastic Layers* Ph D Thesis IIT Delhi (1971)

29 J D Ferry *Viscoelastic Properties of Polymers* John Wiley New York (1980)

30 D I G Jones *J Sound Vib* **140** (1990) 85

31 B C Nakra *The Shock Vib Digest* **8** (1976)

32 B C Nakra *Vibrations of Viscoelastically Damped Laminated Structures* Ph D Thesis (1966)

33 Y V K Sadasiva Rao and B C Nakra *J Sound Vib* **34** (1974) 309

34 R A Di Taranto *J Appl Mech* **32** (1965) 881

35 D J Mead and S Markus *J Sound Vib* **10** (1969) 163

36 D Ross, E E Ungar and E M Kerwin *Colloquim on Structural Damping* ASME (1959) 49

37 B C Nakra and P Grootenhuis *J Engg Ind* **94** (1972) 81

38 N T Asnani and B C Nakra *J Instn Engrs (India)* **50** (1970) 187

39 N T Asnani and B C Nakra *J Engg Ind* **98** (1976) 895

40 D J Mead *J Sound and Vib* **83** (1982) 363

41 M T Yan and E H Dowell *J Appl Mech* **94** (1972) 1041

42 J A Agbasiere and P Grootenhuis *J Mech Engg Sci* **10** (1968) 269

43 D K Rao *J Mech Engg Sci* **20** (1978) 271

44 N T Asnani and B C Nakra *J Aero Soc India* **24** (1972) 288

45 H Oberst *Acustica* **2** (1952) 181

46 J K Dutt and B C Nakra *J Vib Acoust* **115** (1993) 221

47 J K Dutt and B C Nakra *J Sound Vib* **153** (1992) 89

48 J K Dutt and B C Nakra *Mech and Machine Theory* **28** (1993) 427

49 J S Rao *Rotor Dynamics* Wiley Eastern New Delhi (1983)

50 S Shen and K K Stevens *Proc Damping'89* Florida USA (1989)

51 S S A Ravi, T K Kundra and B C Nakra *Proc INCARF* New Delhi India (1993) 639

52 S S A Ravi, T K Kundra and B C Nakra *J Sound and Vib* **179** (1995) 399

53 A K Lall *Optimisation Studies in Viscoelastially Damped Sandwich Beams* Ph D Thesis, IIT Delhi (1984)

54 A K Lall, N T Asnani and B C Nakra *J Vib Acout & Rel Design* **109** (1987) 241

55 R C Johnson *Optimum Design of Mechanical Elements* John Wiley (1980)

56 R Lunden *J Sound Vib* **16** (1979) 25

57 H Eschenauer and H W Wodtke *Optimal Design with Advanced Materials* Elsevier Sci Pub (1993)

58 S S A Ravi, T K Kundra and B C Nakra *Proc IMAC XV* Tokyo (1997)

59 B C Nakra *Proc IUTAM-IITD Winter School on Optimum Dynamic Design* (1997) 187

60 P J Torvik (Ed) *Damping Applications for Vibration Control* ASME AMD-38 (1980)

61 Y Okita and H Okamura *Proc Damping'91 Conf* San Diego, USA (1991) AAC-2

62 S B Choi, B S Thompson and M V Gandhi *Proc Damping '89*, Florida USA (1989) CAC-1

63 A Baz *Proc Damping'93* California USA (1993) IBB-1

64 I Y Shen *J Vib Acoust* **118** (1996) 70

65 R D Cosaro and L H Sperling (Ed) *Sound and Vibration Damping with Polymers* ACS Symp Series (1990)

66 C T Sun and Y P Lu *Vibration Damping of Structural Elements* Prentice Hall New Jersey USA (1995)

67 Z Osinski *Damping of Vibrations* Balkema Rotterdam (1998)

68 D J Mead *Passive Vibration Control* John Wiley Chichester UK (1999)

69 D I G Jones *J Sound Vib* **190** (1996) 449

70 R Singh and B C Nakra *J Sound Vib* **211** (1998) 295

71 B C Nakra *J Sound Vib* **211** (1998) 449

72 L Rogers *Mechanical Engineering* **108** (1986) 66